Procedia Manufacturing

Volume 1, 2015, Pages 779–791

43rd Proceedings of the North American Manufacturing Research Institution of SME http://www.sme.org/namrc

Analysis and Design for Rapid Prototyping Mechanism using Hybrid Flexural Pivots

Jorge Correa and Placid Ferreira
Department of Mechanical Science and Engineering
University of Illinois at Urbana-Champaign. Urbana, IL, USA
jcorre20@illinois.edu, pferreir@illinois.edu

Abstract
High performance motion systems play an important role in modern technology especially in the area of metrology and process equipment related to the field of micro- and nanotechnology. The purpose of this study is to show how to properly design and fabricate prototyped mechanisms that integrate metal-polymer flexural pivots for precision motion applications. Finite element simulations are used to understand the mechanical behavior of these components leading to dimensions that minimize the work done by the polymer structures. Simulations indicate that, the penetration distance of the metallic inserts into the polymer structures should be around one half of the total insert length and that the profile of the pressure interference can be modified to enhance the performance of the composite structure. A cantilever beam with a flexural pivot is used to test the performance of the design and a piezoelectric-actuated four bar mechanism is prototyped and studied as a general application of these types of structures to the precision motion field. The methodology implemented in this work poses a simple and affordable way to fabricate, assemble and customize low-cost devices for precision motion application and it applies to both, systems fabricated by polymer and metal rapid prototyping technologies.

Keywords: Hybrid flexural pivots, flexural systems, prototyped mechanisms

1 Introduction

Flexure based mechanisms are of great importance in modern technology application fields such as micro and nanopositioning, trajectory scanning and several probe/tool based metrology. A flexure is a compliant element that provides relative motion between adjacent rigid members through controlled flexing. They are particularly relevant to precision engineering because of their ability to amplify or attenuate a mechanical input in a repeatable and controlled way (Howel, 2001), (Lobontiu, 2003). Conventionally, flexure-type systems are manufactured from high performance metals such as

Peer-review under responsibility of the NAMRI Scientific Committee
doi:10.1016/j.promfg.2015.09.062

Fig. 1. A commercial cantilevered design of a cross axis flexural pivot.

stainless and alloyed steel or aluminum alloys for high material performance and durability (J.Dong, 2008) (Dong, 2008) (Culpepper & Anderson, 2004) (Dunning, et al., 2012.) (Shorya & Slocum, 2005). Functional requirements such as high bandwidth, accuracy performance and geometric complexity require them to be manufactured as monolithic structures using conventional precision machining and electro discharge machining (EDM). However, such an approach is expensive and not practical for mass production. They can only be used for custom and high-value added applications. More recently, rapid prototyping technology (RP) has been proposed and implemented in the fabrication of cost-effective flexure-based mechanisms with complicated spatial structures (Alok & Rosen, 2001.) (Constantinos, et al., 2001) (Hod, et al., 2005.) (Laliberte, et al., 2001.) (Yonghua & Chen, 2011.). Some of the advantages of using rapid prototyping in the fabrication of flexure-based mechanisms are: quick product testing, ease-of-design iteration, elimination of design errors, workspace validation, evaluation of singular configurations and link interference determination. However, the reported limitations are: dimensional accuracy, low quality surface finishing, anisotropic prosperities, thermal instability, holding force capabilities. Severely reduced durability of the flexural elements as most rapid prototyped materials are unsuitable in fatigue loading is a particularly debilitating drawback.

We envision an approach that uses economic methods like casting and molding (for high volume production) and 3-D printing (for custom, one-off systems) for manufacturing the complex geometry of the structural parts of the systems, flexural elements of simple geometry with specialized materials (e.g. spring steel, etc.), and well-design interfaces between the two. This paper presents a design methodology for prototyped mechanism with hybrid-flexural pivots and proposes a process for their

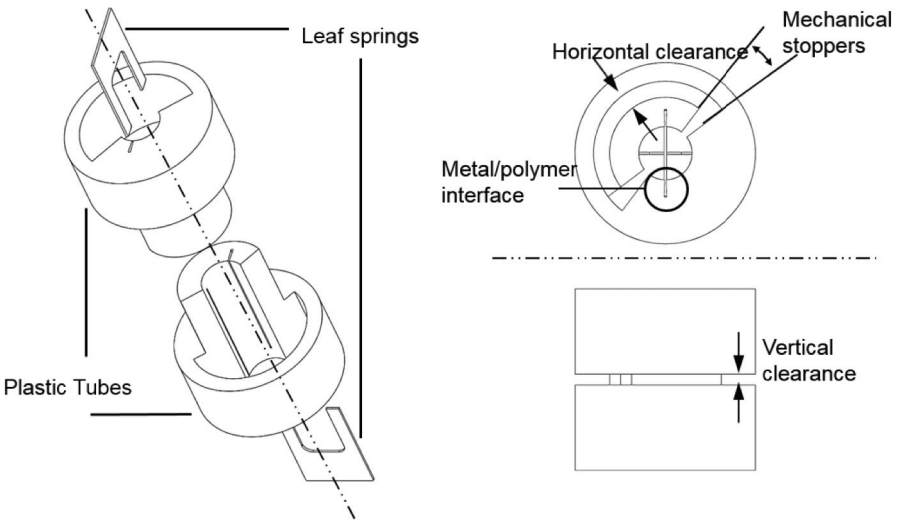

Fig. 2. Assembly of a cross axis flexural pivot.

fabrication. In this study, finite element simulations are used to understand the mechanical behavior of these elements and to produce optimal design for the aforementioned interfaces between components. In the proposed fabrication process, the links in device structure are prototyped as a single monolithic piece, held together by sacrificial structures or tabs. This is followed by the insertion of metallic leafs, press-fitted into place to complete what we call the hybrid flexural pivots. The hybrid pivots, in the designs described here, allow for relative rotations between the different links of the mechanism. Finally, the holding or sacrificial tabs are snapped off and the devices are ready for operation. This methodology combines the ability and effectiveness of Rapid Prototyping in economically creating complicated spatial structures with the superior mechanical properties of metallic inserts, necessary for the flexural components. This provides numerous advantages for the design of precision motion systems such as: (a) rapid and affordable customization, (b) rapid fabrication, (c) time and cost saving, and (d) designs that are suitable for light-weight applications.

An important aspect of this design and fabrication strategy is the interface between the rigid links (which might be made of many different materials including polymers, additively deposited metals, and cast metals) and the flexural elements. The joints that result are what we refer to as hybrid flexural pivots. Section 2 of this paper establishes the design goals of the hybrid-flexural pivots. Section 3 provides simple analytic models to evaluate the load-deflection behavior of conventional flexural pivots as a first design approach to estimate the general dimensions. Section 4 and 5 explore the fabrication issues and the integration schemes of hybrid-flexural pivots into the prototyped structures. Experimental validation of this work is presented in section 7.

2 Problem definition

Flexural pivots are compliant joints designed to produce limited relative rotation between two coaxial, split tubes. The tubes are attached to each other by means of flexural leafs that allow the rotation of one with respect to the other through flexing. Ideally, flexing takes places about the midpoint of the flexural leaves attaching the tubes. Figure 1 shows a commercial design of a cantilevered cross-axis flexural pivot (Lobontiu, 2003).

This work presents a methodology on how to design the interface between the flexural leaves and the tubes (in this case, made from a polymer with a rapid prototyping process). The pivots are design to have constant stiffness, minimum parasitic motion and behave elastically throughout their range of motion. The design criterion focuses on the load/deflection characteristics of this machine component and the mechanical interactions at the metal/polymer interface. FEM (finite element method) structural analysis is used to understand these interactions. A brief description of the pin-joint model (Jensen & Howell, 2002) (presented on section 3.1) is used as a first design approach to estimate the flexural pivots stiffness.

3 Methodology

The hybrid flexural pivot of this work are made of two cylindrical pieces (embedded into the prototyped mechanisms) that are attached to each other by metallic leafs. The leaf springs can be manually press fitted through vertical grooves along the polymer cylinders. Initially, the tubes are held together by polymer tabs that are snapped off after the insertion of the springs. Fig. 2 shows an exploded view of the hybrid cross-axis flexural pivot. Some of the critical design-parameters of the hybrid pivots are the vertical and radial clearances between the polymer cylinders, used to avoid contact during the motion of the joints. Mechanical stoppers are also included in the design to prevent mechanical failure of the components by imposing a maximum angle of rotation.

3.1 The pin-joint model for cross-axis flexural pivots

In the pin-joint model by Jensen and Howell (Jensen & Howell, 2002), one can conceptually think of the joint as having a rigid pin located at the center of the flexural pivot, shown in Fig. 3. Then, we have the joint stiffness given by:

$$K = \frac{K_\theta EI}{2l}$$

Where K is the rotational stiffness of the pivot, E is the Young's modulus of the material and I is the moment of inertia of the flexible section and l is the length of the flexible segments. K_θ is regarded as the stiffness coefficient and it is a function of the dimensionless parameter n defined as the ratio of the effective pivot length r and the in-plane pivot width h (see Fig. 3)**.** To use the pin-joint model, the value of the stiffness coefficient K_θ needs to be determined first. K_θ is determined by minimizing the deflection error of the cross-axis flexural pivot through a motion of 1.1 radians for different values of the dimensionless parameter, n. Afterwards, a polynomial curve fit is used, yielding the function. The authors report the following polynomial equation for the value of K_θ;

$$K_\theta = 5.300185 - 1.6866n + 0.885356n^2 - 0.2094n^3 + 0.018385n^4$$

With $0.5 \leq n \leq 4.0$. To exemplify the methodology, the flexural pivots of this work have dimensions t = 0.254 mm, l = 5 mm and width w = 5mm. Then, the parameter n equals 1. The material used is steel with Young's modulus E = 200 GPa and a proportional limit of 480 MPa. A metal flexural pivot with these materials and dimensions has a rotational stiffness coefficient K_θ = 4.30792 and rotational stiffness K = 0.5767 N m/rad. Here, we used the pin-joint model as an initial criteria to estimate the dimensions of the hybrid cross-axis flexural pivots such as length, thickness and width of the springs as well as to evaluate its load-deflection characteristics.

3.2 A Finite Element Model of Hybrid-Flexural-Pivots

Our FEA model is a two dimensional abstraction of a hybrid flexural pivots under the action of a counter-clock wise torque applied to one of its ends. Fig. 3 presents the schematics and critical dimensions of this model. Each leaf spring has an effective length l and a thickness t. The springs penetrate the polymer structure to a depth, d. The simulations were implemented in Abacus CAE as a plain elastic problem with a constant thickness w and a hard contact interaction between the polymer and the metallic elements. The material used for leafs is steel with Young modulus E_m = 200 Gpa and Poisson coefficient ν_m = 0.33. The polymer structure was modeled as an ABS polymer with Young modulus E_p= 2.9 MPa and Poisson coefficient ν_p = 0.44.

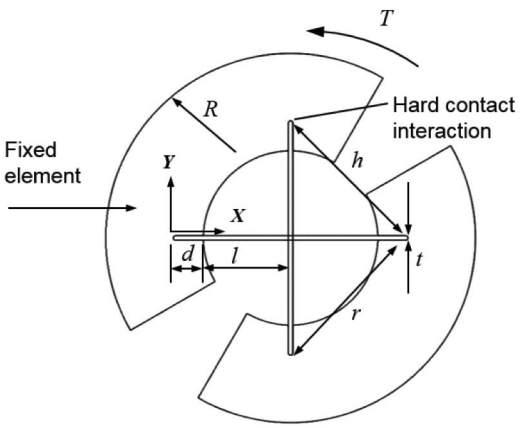

Fig. 3. Plain strain simplification of a hybrid leaf spring.

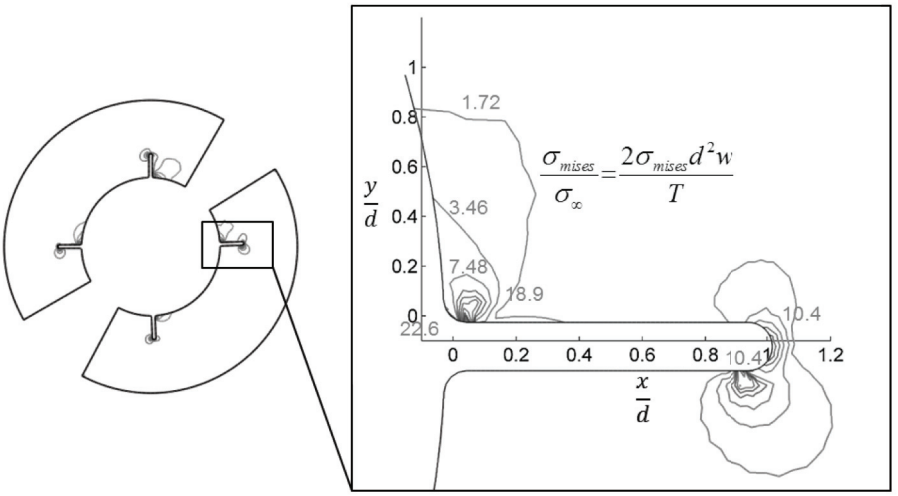

Fig. 4. Plain strain simplification of a hybrid leaf spring.

Fig. 4 shows the Von Mises stress distribution normalized by the nominal stress at the interface near the polymer grooves. The nominal stress at the interface is defines as

$$\sigma_\infty = \frac{T}{2d^2 w}$$

This equation results from evenly distributing the reaction forces, due to the external torque, along the area of the interface. The X-Y coordinates are also normalized by the penetration distance *d*. The Von Mises stress field reveals that there are two main causes of stress concentration at the interface, namely, the localized contact pressure between the leafs and the polymer structures at opposite sides of the interface and the stress distribution at the tip of the notch resulting from the opening of the groove. The high concentration of stresses at the interface results in a significant amount of the motion in pivot due to the compliance of the polymer structure. The following section proposes a criterion to find the optimum penetration distance in which the compliance of the polymer notch and the energy stored in the polymer structure are minimized during the motion of the pivot.

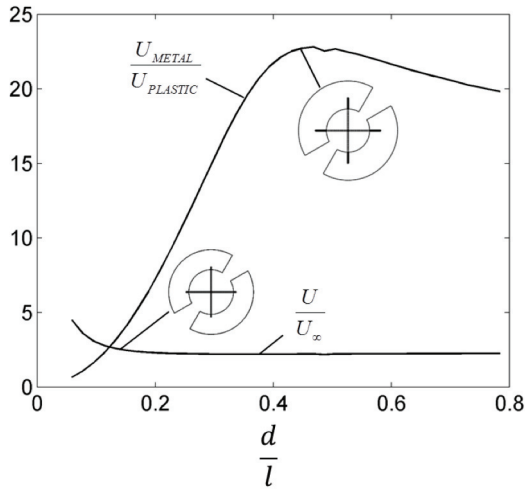

Fig. 5. Strain energy distribution as a function of the ration *d/l*.

3.3 Determining the leaf penetration distance

To optimize the performance of the flexural pivot, we consider the mean compliance and its relation with the strain energy stored in the system. Fig. 5 shows the total strain energy stored in the system normalized by the strain energy of a conventional pivot with the same dimensions and loading. The normalized energy is computed as:

$$U_{\infty} = \frac{K\theta^2}{2} = \frac{K_{\theta} E_m I_m \theta^2}{4l}$$

The ratio of the energies stored in each of the components is also plotted as a function of the ratio *d/l*. From the graph it is observed that when the penetration distance is grater that 20% of the effective leaf length, the total strain energy the system U, is minimum and has a constant value of $2.2U_{\infty}$, this factor corresponds to the extra compliance introduce by the polymer structure in the pivot. At this point the extra-compliance of the systems has been minimized. However, a more beneficial distribution of the potential energy stored in the system can be obtained by controlling the ratio of strain energy stored in the polymer and metallic components. For a penetration distance close to 50% of the effective leaf length, the metallic components store about 22 times more energy the polymer components, thus, suggesting an optimal design point for the structural integrity of these elements. At higher penetration depth, the compliance of the notch structure becomes significant resulting in a higher value of energy stored in the polymer components.

3.4 Designing an interference fit at the metal-polymer interface

The localized pressure at opposite locations of the interface can be attenuated by pre-stressing the interface using an interference fit between the polymer notch and the metallic leafs. The amplitude of the pressure distribution in the interface increases with the value of the interference fit. Fig. 6 shows the simulated pressure distribution at the interface for the cases of zero and 15 μm interferences when the pivot is twisted an angle of 1 degree. The pressure at the interface has been normalized by the nominal stress for both cases. From the graph, it can be observed that a properly design interface can attenuate the stress concentrations by distributing the stresses along the length of the notch and can also prevent delamination during the motion of the pivot. Delamination of the interface takes place whenever the pressure at any sides of the interface drops to zero. These results suggest that the interference distance can be modified to meet the motion requirements avoiding delamination and high stress concentrations.

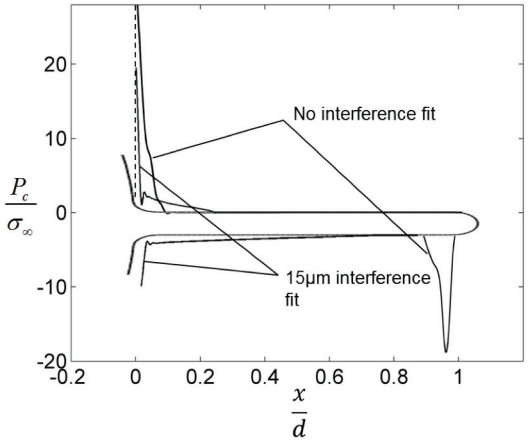

Fig. 6. Pressure at the interface for a rotation of 1 degree as a function of the ration *d/l*.

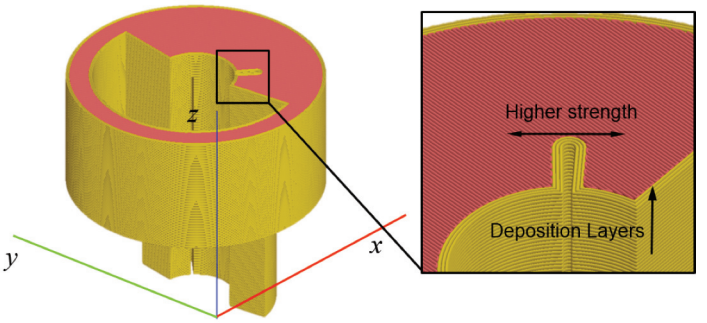

Fig. 7. Example of sliced part oriented properly

3.5 Rapid prototyping assembly and testing of the polymer-metal joint

Because of the anisotropy of the material deposited layer by layer, the parts must be properly oriented to achieve the desired strength near the contact interfaces (Fig. 7). Deposition layers oriented orthogonal to the leaf axis of rotation, increase the strength of the plastic structure in the directions of the tractions transmitted by the inserts. The assembly of the joint is achieved using a manual press, with vertical forces around 2.5 Kg .The dimensional accuracy and surface finish of the mating surfaces are important fabrication considerations that pose a challenge to the SLA process. The flexural pivots were adapted for fabrication using the ViperTM SLA system. Given the machine capabilities (layer thickness of 25 µm in high resolution mode), it is difficult to achieve smooth-vertical surfaces and repeatable interferences of less than 100 µm of overlap between the metal insert and the plastic parts. However, the approach presented in this work can be transferred to the growing Direct Metal Laser Sintering (DMLS) technology, which produces stronger and denser parts that allow for higher interference dimensions corresponding to tighter contact pressures. This is beneficial both to the assembly process and to reduce backlash in the joint during operation. This design methodology can also be extended to mass production using low-cost manufacturing process with higher control capabilities such as casting and molding.

To produce functional plastic-metal joints, previously EDM metallic springs were inserted into different SLA parts in a trial and error process using SLA materials water clear Ultra 10122 and ProtGenTM O-XT 18420 (Fig. 8). Although, the parts made of water clear Ultra10122 exhibited better dimensional accuracy, the ProtGen is a more suitable choice for this application due to its better toughness. The trial and error process resulted on an interference fit of 50 µm and vertical and radial clearances of 1 mm and 1.5 mm respectively.

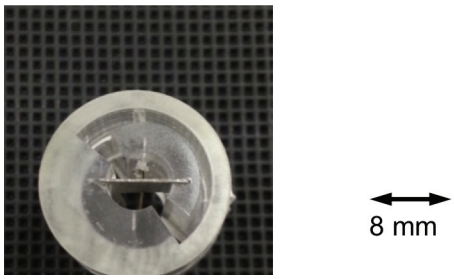

Fig. 8. Assembly of a hybrid flexural pivot using SLA water clear material

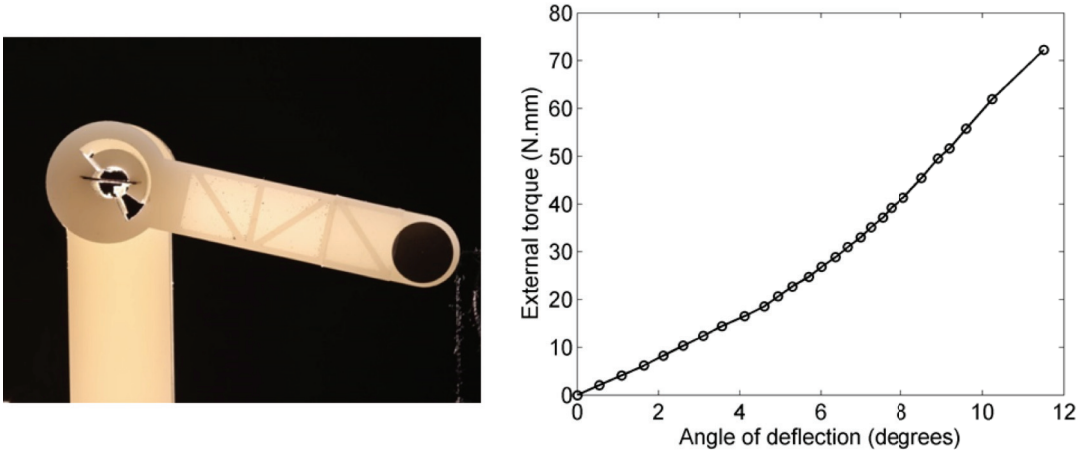

Fig. 9. A prototyped cantilever beam with a hybrid flexural pivot and its load-deflection behavior

To test the load-deflection of the design components, a cantilever beam with a flexural pivot acting as torsional spring was prototyped. A picture of the setup is shown in Fig. 9. The critical dimensions of the design are the same of Sec. 3.5. The length of the cantilever arm is 50 mm. To obtain the load-displacement behavior, different weights with incremental values ranging between 1g and 20g were sequentially attached to the end-tip of the cantilever. The corresponding values of deflection were extracted by capturing images at the equilibrium configuration. The measured data was post-processing using image software to correct for the registration issues in the setup. Fig 8 also presents the load deflection characteristics of the system. It can be seen form the graph that the flexure stiffness starts with an initial value of 0.1375 N.m/rad for smaller angles of deflection; as the twist angle increases, the flexural pivot stiffness increases to a value of 0.5913Nm/rad. The change in stiffness suggests the existence of backlash between the insert and the polymer structure due to the low tolerance control in the SLA process. The play prevents the elements of the joint from fully engaging during the early stages of motion.

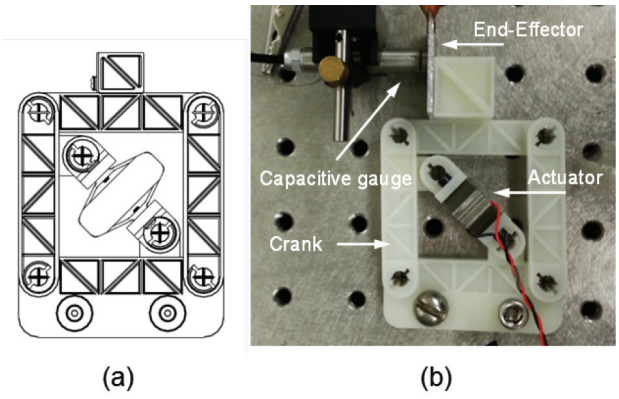

Fig. 10. (a) CAD model and (b) prototype of piezoelectric actuated mechanism

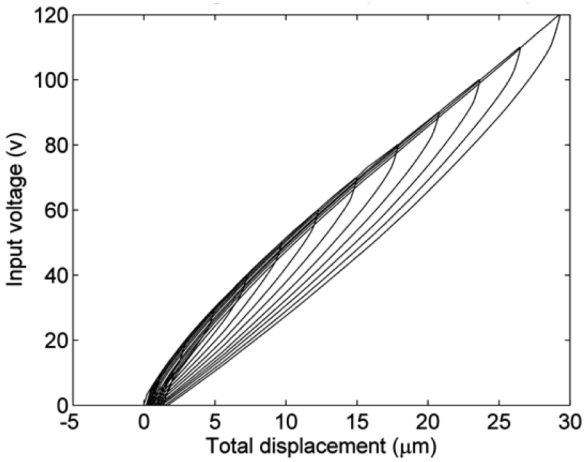

Fig. 11. Voltage-displacement plots for piezoelectric actuated mechanism.

4 Application: Piezoelectric Actuated Mechanism

To demonstrate the versatility of this design, a piezoelectric-actuated parallelogram four-bar mechanism embedded, with hybrid flexural pivot joints was prototyped, assembled and tested (Fig. 10). A piezoelectric actuator was chosen because of its size, bandwidth and actuation force capabilities. For the sake of compactness, the actuator is assembled inside the parallelogram with the line of actuation making an angle of 45 degrees with the crank and the follower. To reduce the bending torque experienced by the actuator, it is mounted between two flexural pivots that are attached to the crank and to the base of the device. The mechanism consists of six flexural pivots each of them having two metallic leaf springs. The solid model and the prototype version of the mechanism with the actuator connected are shown in Fig.9. The chosen actuator is a CEDRAT APA40, with free stroke 52 μm, blocking force of 194N and a maximum driving voltage of 150V. The chosen dimensions for the crank and follower were 45 mm. The end effector has a total displacement of 28 μm corresponding to a rotational range of the hinges of 0.04 degrees. For this ranges of angular displacement, the loss of parasitic motion in the vertical direction are 1.12 nanometer and the changes in angular stiffness of the hybrid joints are negligible. Capacitive sensors (Probe 2805 and Gauging Module 4810 ADE Technologies) are used to directly capture the motion of the end effector. The target for the capacitive sensor is a polished aluminum plate glued to the end-effector of the four bar mechanism.

4.1 Static response

To study the static behavior of the device, the input voltage to the actuator was sequentially ramped up at increasing values, from 0 volts to 120 volts in increments of 10 V, and plotted against the end-effector motion observed by the capacitive sensor. The signal was generated at a low frequency (0.015 Hz) to rule out the dynamic effects. The results of this experiment are reported in Fig. 11. For the small angular displacement of the hybrid pivots, the hysteresis and loss of motion in the system are due to the piezoelectric actuator rather than the mechanical response of the structure. This hypothesis was validated by carrying out the same experiment with the piezoelectric actuator disengaged from the mechanism.

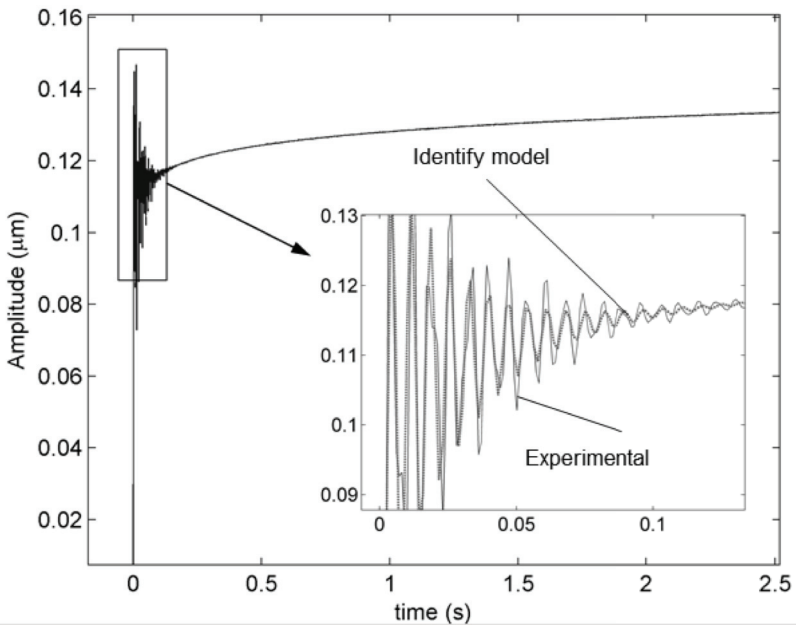

Fig. 12. Step response of piezoelectric actuated 4-bar mechanism

4.2 Dynamic response

To capture the dynamics of the system, a step input of 1 volt was introduced to the actuator while the position of the end-effector was recorded by the capacitive sensor. Fig. 12 shows the step response of the system. The identified damped natural frequency for the system is 140 Hz. To gain further understanding of the dynamics of the system, the Bode plot of the open-loop response was generated using a dynamic signal analyzer. Figure 13 shows the amplitude and phase diagrams when the input frequency is sweep between the values of 5 Hz and 1000 Hz near to the equilibrium point, at a constant amplitude of 4 V. The experimental data shows that the damped resonant frequency of the system is consistent with the 140 Hz of damped natural frequency obtained from the step response. The frequency response also indicates that the open-loop bandwidth of the system is 50 Hz as the gain and the phase lag of the system remain constant below this value. A transfer function of the system

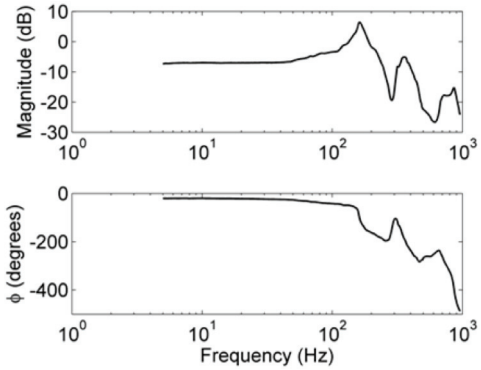

Fig. 13. Frequency response of piezoelectric actuated 4bar mechanism

was identified using both the experimental step input and frequency response as:

$$G(s) = \frac{-0.06031S^2 + 243.8S + 154.6}{S^2 + 517.6S + 277.2}$$

The zeros in the system account for the hysteretic behavior of the piezoelectric actuator. The experimental and identified step responses of the system are shown in Fig. 12.

4.3 Closed-loop tracking performance

Tracking performance and contouring accuracy are central characteristics for micropositioning systems. To test the performance of the prototyped mechanism a PI controller was designed based on the experimental observation of the system. In a trial an error methods in which the proportional action was the main control, the integral action was used to refine the tracking performance. This procedure resulted in. The controls of the device were implemented using a D-space motion controller. Fig 14. shows the close loop scheme for the PI controller. In this scheme, sine waves of different frequencies were generated with the D-space controller and used as reference signals. The reading form the capacitive sensor was used as feedback and the error between the reference and sensing signals was used as the input for the PI controller. A DAC systems together with an amplifier were used to convert the controller signal to the analog voltage ranges of the piezoelectric actuator and to digitalize the reading from the capacitive sensor back to the controller. Tracking tests were conducted by driving the mechanism along a sinusoidal trajectory with amplitude of 5 um an top speeds ranging from 0 to 80

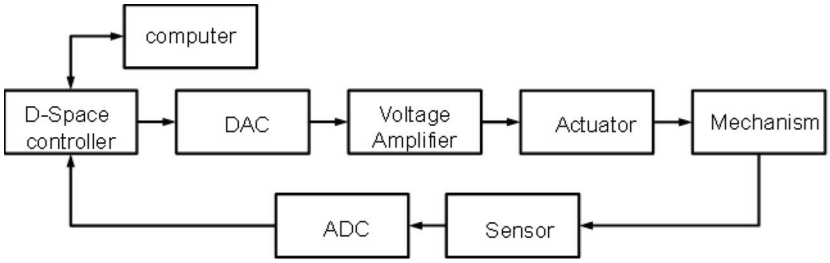

Fig. 14. Close loop control scheme

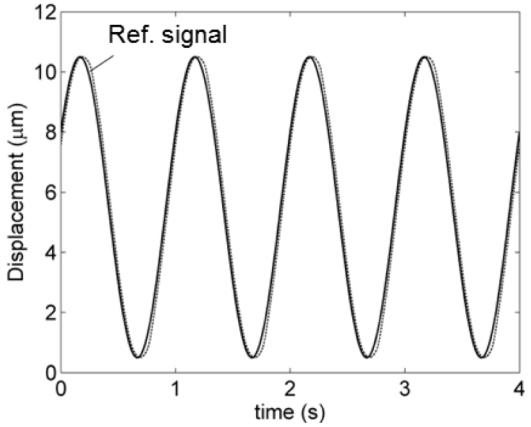

Fig. 15. 4bar mechanism tracking performance

um/s. Fig. 15 shows the time response of the system at a driven speed of 80 μm/s . The results of the sinusoidal tracking test are summarized in table 1. The maximum tracking error at 80 um/s is less than 180 nm and the average contouring error is less than 50 nm.

5. Conclusions

This paper presents a design methodology for prototyping mechanisms with hybrid flexural pivots. Here, the pin-joint model was referenced as initial design criteria for the critical dimension of these elements. Detailed FEA analysis on the interface between the metallic and polymer components revealed two main mechanisms of stress concentration, namely, the localized contact stresses and the notch tip stresses. A criteria based on the strain energy distribution was proposed to reduce the intensity of the stress fields and the amount of work done by the polymer structure during the motion of the pivot. This resulted in a suggested penetration leaf penetration depth into the polymer equal to one half of the total insert length. An interference fit was also shown as an approach to attenuate and distribute the otherwise localized contact stresses, thus preventing delamination at the interface. Experimental setups of a single flexural pivot and a parallelogram 4-bar mechanism were presented to

Table 1. Sinusoidal tracking results

Max. Speed (um/s)	Max. error (nm)	Average error (nm)
20	32.6	17.8
40	164.1	19.1
80	169.4	38.2
160	176.4	42.7

show the validity and performance of this type of an approach for realizing micro-and nanopositioning devices.

References

Alok, K. & Rosen, D. W. (2001). Building around inserts: methods for fabricating complex devices in stereolithography.. *Rapid Prototyping Journa,* Volume 7(5), p. 253–262.

Constantinos, M., Kathryn, J. D., Jey, W. & Munshi, A. (2001). Fabrication of nonassembly mechanisms and robotic systems using rapid prototyping. *Joural of Mechanical Design,* Volume 123, p. 516.

Culpepper, M. L. & Anderson, G. (2004). Design of a low-cost nano-manipulator which utilizes a monolithic, spatial compliant mechanism.. *Precision engineering,* Volume 28(4), p. 469–482.

Dong, J., Ferreira, P. (2008). A novel parallel-kinematics mechanisms for integrated, multi-axis nanopositioning Part 1. Kinematics and design for fabrication. *Precision Engineering 32 (2008) 7–19,* p. 32 7–19.

Dunning, A., Tolou, N. & Herder, J. (2012). A compact low-stiffness six degrees of freedom compliant precision stage.. *Precision Engineering.*

Hod, L., Francis, C. M., Jimmy, H. & Carlo, P. (2005). 3-d printing the history of mechanisms.. *Journal of Mechanical Design, ,* Volume 127, p. 1029.

Howel, L. (2001). *Compliant Mechanisms.* New York: Wiley.

J.Dong, Ferreira, P. (2008). A novel parallel-kinematics mechanism for integrated, multi-axis nanopositioning Part 2: Dynamics, control and performance analysis.. *Precision Engineering 32 (2008) 20–33,* p. 32 20–33.

Jensen, B. D. & Howell, L. L. (2002). The modeling of cross-axis flexural pivots. *Mechanism and machine Theory,* Volume 37, pp. 461-476.

Laliberte, T., Gosselin, C. M. & Cote, G. (2001). Practical prototyping.. *Robotics & Automation Magazine, IEEE,,* Volume 8(3), p. 43–52.

Lobontiu, N. (2003). *Compliant mechanism: design of flexures hinges.* s.l.:CRC press.

Shorya, A. & Slocum, A. H. (2005). Topology evolution of high performance xy flexure stages.. *In Proc. ASPE Annual Meeting, Norfolk, VA, Paper,* p. 1802.

Yonghua, C. & Chen, Z. (2011). Joint analysis in rapid fabrication of non-assembly mechanism.. *Rapid Prototyping Journal,* Volume 17(6), p. 408–417.